Imperfect Fabry-Perot resonators

Klaassen, T.

CHAPTER 3

Transverse mode coupling in an optical resonator

Small-angle scattering due to mirror surface roughness is shown to couple the optical modes and deform the transmission spectra in a frequency-degenerate optical cavity. A simple model based on a random scattering matrix clearly visualizes the mixing and avoided crossings between multiple transverse modes. These effects are only visible in the frequency-domain spectra; cavity ring-down experiments are unaffected by changes in the spatial coherence as they just probe the intra-cavity photon lifetime.

T. Klaassen, J. de Jong, M. P. van Exter, and J. P. Woerdman, Opt. Lett. **30**, *1959-1961 (2005).*

3.1 Introduction

Optical resonators are used in many experiments; they provide for high resolution in optical interferometry and for field enhancement in QED experiments [4]. At specific "magic" resonator lengths many transverse modes of the resonator have the same eigenfrequencies [12, 21]. Such frequency-degenerate resonators have been suggested as a tool to enhance the efficiency of removing entropy from atoms (cooling) in a resonator [36] and to observe cavity-enhanced spontaneous emission at optical wavelengths [37].

Although loss due to scattering by mirrors is well-known for optical cavities [16, 22], the special role of frequency-degeneracy in scattering is only touched upon in the literature [38] and no systematic study has been performed. In this Chapter, we demonstrate that at frequency-degeneracy it is the *amplitude* scattering instead of the *intensity* scattering that matters and show that the observed difference between time and frequency-domain measurements around frequency-degeneracy is caused by mode-mixing of many transverse modes. The coupling (due to surface roughness of the mirrors) changes the eigenmodes and eigenfrequencies, which no longer coincide at frequency-degeneracy. This results in an inhomogeneous broadening of the measured resonances.

3.2 The experiment

In our experiment, a laser beam at fixed wavelength ($\lambda = 532$ nm) is injected into a symmetric stable (Fabry-Perot) cavity to match its TEM_{00} mode. The cavity is constructed with two nominally identical highly reflective mirrors (specified reflectivity $> 99.8\%$), having a radius of curvature of $R = 50$ cm and a diameter of $D = 5$ cm. We operate the cavity close to a frequency-degenerate point, where the eigenfrequencies of the Hermite-Gaussian (HG) eigenmodes separate into N groups of almost frequency-degenerate modes. At frequency-degeneracy, the Gouy phase θ_0, being the round-trip phase delay between the fundamental HG mode as compared to a reference plane wave, is by definition a rational fraction of 2π: $\theta_0 = 2\pi/N$, the paraxial phase delay of higher-order modes (TEM_{mn}) being $(m+n+1)\theta_0$ [12]. In a ray picture of a frequency-degenerate resonator, the ray path closes itself after N (equal to the number of hit points on each mirror) round-trips inside the resonator [21]. For stability reasons, we avoided the popular confocal ($N = 2$) configuration [12]. By way of example, we restrict the discussion to $N = 4$, this corresponds to a cavity length $L = 14.6$ cm at $R = 50$ cm.

We measure transmission spectra by scanning the cavity length L over a few wavelengths with a piezo element. From these spectra we deduce the cavity finesse F as the ratio between the free spectral range $c/(2L) = 1.03$ GHz and the (FWHM) width of the dominant transmission resonance. Fig. 3.1 shows the finesse as a function of the cavity length, which can be accurately adjusted with a translation stage. Note, how the finesse drops from 1300 to 600 around frequency-degeneracy over a range (FWHM) of $\delta = \Delta L/R = 4.3 \times 10^{-4}$. This range corresponds to a frequency difference $\Delta\nu = 0.78$ MHz between consecutive classes of transverse modes ($\Delta(m+n) = N = 4$). The inset shows that the resonance width more than doubles and that the corresponding peak transmission is reduced to below 50% for spectra at $\delta = 0$ as compared to $\delta = -1 \times 10^{-3}$.

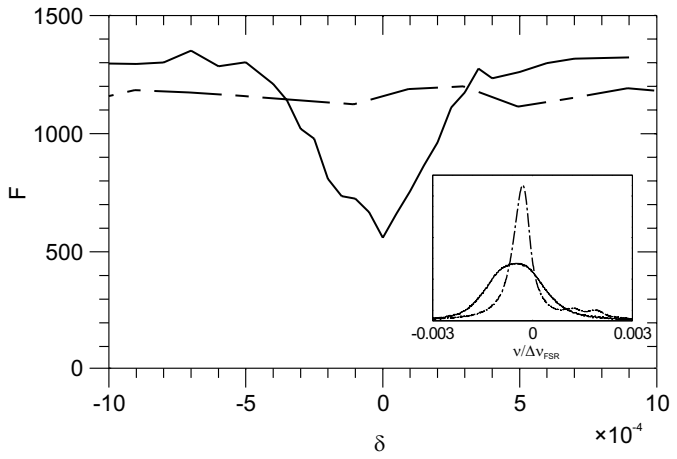

Figure 3.1: *Relative spectral width of cavity resonances, expressed as the finesse F, measured as a function of the normalized cavity length δ, for a resonator with (dashed) and without (solid) a centered intra-cavity pinhole. The inset shows two typical spectra measured at $\delta = 0$ (solid) and $\delta = -1 \times 10^{-3}$ (dashed).*

We attribute the observed drop in finesse to mode coupling induced by scattering at the (imperfect) mirrors. A proof of this statement is given by the dashed curve in Fig. 3.1, which shows the measured finesse for the same cavity with a pinhole centered in the middle of the cavity; *this* finesse is constant over the full range. The intra-cavity pinhole (diameter 1 mm; waist of TEM_{00} mode 0.17 mm) basically converts our multi-transverse-mode system into a single-mode system, by increasing the losses of the higher-order transverse modes and reducing the mode coupling. It thereby removes the mode mixing that caused the finesse reduction and makes the system essentially single transverse mode.

The cavity finesse can also be determined with a cavity ring-down experiment, which measures the intra-cavity photon lifetime after switching-off the optical injection [39, 40]. We have performed this experiment (without intra-cavity pinhole) with a sufficiently large detector over the same detuning range and found absolutely no differences at or away from degeneracy. From the measured lifetime of $\tau \approx 0.35$ µs, we obtained a constant value of $F \approx 2200$ over the full range (we do not have an explanation why this value is different from the value $F = 1300$ mentioned above).

Cavity ring-down experiments are insensitive to the power distribution over the transverse modes unless one uses an (extra-cavity) pinhole in front of the optical detector [39, 40]. By passing only a fraction of the amplitude mode profiles, the transmitted power can then reveal beatings between transverse modes that are only orthogonal over their *full* profile. Using this configuration at the degenerate cavity length ($N = 4$), we experimentally observed that the decay becomes nonexponential and, depending on the position of the detector pinhole, can be either faster or slower than the decay observed without pinhole. The obvious conclusion is that we observe the decay and beating of several (nondegenerate) transverse modes that are simultaneously excited by an injection profile that was matched to just a single TEM_{00} mode.

Theoretically, the optical field at any plane in the resonator can be described by separating

it in transverse spatial eigenmodes j and amplitudes that change in time

$$E(x,t) = \sum_j a_j(t) u_j(x) \; . \tag{3.1}$$

This evolution is trivial if we assume that all modes have equal loss rates Γ, as should be the case for low-order transverse modes and large mirrors. In a cavity ring-down experiment the spatially integrated intensity decays then with a rate 2Γ. In a spectral measurement, where one scans either the laser frequency or the precise cavity length, a large-area detector will measure

$$P_{\text{out}}(\omega) \propto \sum_j |a_j(\omega)|^2 \propto \sum_j \frac{\left| \int E_{\text{in}}(x) \cdot u_j^*(x) dx \right|^2}{(\omega - \omega_j)^2 + \Gamma^2} \; , \tag{3.2}$$

where the numerator quantifies the spatial overlap between the injected field $E_{\text{in}}(x)$ and the eigenmodes and the denominator quantifies the corresponding spectral overlap.

The key argument we want to make is that the shape of the eigenmodes $u_j(x)$ can be quite different from the usual (HG) shape in a cavity that operates close to frequency-degeneracy. The reason is that even a small amount of scattering at the mirrors can lead to dramatic changes in the modal profile if it can resonantly perturb the mode profile over and over again on consecutive round-trips. A similar phenomenon is known in quantum mechanics, where energy-degenerate perturbation theory is quite different from nondegenerate perturbation theory, which gives second-order expressions that explode at degeneracy as they are inversely proportional to the energy differences between the unperturbed modes.

3.3 Simulations

To find the true eigenmodes in a perturbed cavity we use the observation that the optical field inside a cavity can be described by a Schrödinger-type equation [41]. We take the simplest form of coupling, which is found in many physical systems, and model it with a random matrix $\mathbf{c}$ of the GOE class [42]. In the basis of the unperturbed HG-modes, the matrix equation for the eigenfrequencies ω_j and eigenmodes $\mathbf{u}_j$ of the coupled system is thus

$$\omega_j \mathbf{u}_j = M \mathbf{u}_j = \begin{pmatrix} c_{00} & c_{01} & c_{02} & \dots \\ c_{10} & \varepsilon + c_{11} & c_{12} & \dots \\ c_{20} & c_{21} & 2\varepsilon + c_{22} & \dots \\ \vdots & \vdots & \vdots & \ddots \end{pmatrix} \mathbf{u}_j \; , \tag{3.3}$$

where ε is the frequency detuning away from degeneracy. The coupling matrix $\mathbf{c}$ is random but fixed for each realization of the system, with coefficients that are normalized via their statistical variance $\langle c_{ij}^2 \rangle = 1$. Energy conservation is assured via $c_{ij} = c_{ji}^\dagger$ and is physically motivated by the observation that the scattering due to mild surface roughness produces so-called conservative coupling [41]. The amplitudes of the HG modes evolve via the same matrix M as in Eq. 3.3.

For simplicity, we have reduced the transverse dimensionality from 2 to 1, by grouping HG_{nm}-modes with the same $n+m$ value and unperturbed eigenfrequency into families

$j = (n+m)/N$, and assume equal coupling between these families. On the one hand, the coupling amplitudes between the individual modes will decrease with increasing mode number difference, as small-angle scattering due to gradual variations of the mirror height profile generally dominates over large-angle scattering [29]. On the other hand, the coupling between mode families will increase with mode number as the number of modes per family also increases. For simplicity again, these counter-acting phenomena are assumed to balance.

The white curves in Fig. 3.2a show the calculated eigenfrequencies as a function of the detuning ε for 10 eigenmodes. Far from degeneracy, the on-diagonal elements of M dominate the dynamics, the eigenmodes closely resemble the HG-modes with equally-spaced eigenfrequencies $j\varepsilon$. Around degeneracy, mode mixing occurs and the eigenvalues exhibit a "10-mode" avoided crossing, with "level repulsion driven chaos" [42] as central at $\varepsilon = 0$. Whereas the white curves show the eigenfrequencies of all modes, the underlying picture is sensitive to the overlap with the injection mode, making some (lower-order) modes visible around degeneracy, whereas others are barely excited. Fig. 3.2a has been obtained by assuming a damping rate $\Gamma = 1$ to produce finite spectral widths and a realistic injection profile $E_{\mathrm{in}}(x)$ that is matched to the fundamental HG mode. Note how the almost single-mode excitation away from degeneracy unavoidably decomposes into many (modified) eigenmodes at degeneracy.

Fig. 3.2b shows a composite plot of the measured transmission curves as a function of the normalized cavity length δ, which can be transformed into a frequency detuning via $d\varepsilon/d\delta \approx Nc/[2\pi L\sin(\theta_0/2)] = 1.84$ GHz. We dominantly excite the TEM_{00}; the intensity ratio of the TEM_{04} and TEM_{00} is only 5%. Note that close to frequency-degeneracy $\delta = 0$ the peak transmission reduces and the resonance broadens due to mode-mixing, as shown previously in Fig. 3.1. The results of our model are in nice agreement with the measurements.

For a qualitative comparison between the mirror surface roughness and the mode coupling, we note that the amplitude of the roughness is directly proportional to the coupling amplitude c_{ij} between modes. The spatial frequency of the roughness determines the scattering angle or equivalently the TEM_{mn}-mode to which the scatter couples; the system is particularly sensitive to spatial frequencies in the order of the inverse beam size (0.17 mm). A rough estimate of the scatter *amplitude* c_{ij} is given by the ratio of the locking range over the free spectral range, being 8×10^{-4} (roughly equal to the scaling between Fig. 3.2a and b). Away from frequency-degeneracy the system feels only the scatter *intensity* which is less than 10^{-6} per mode.

From a general perspective, the time and frequency domain measurements of the cavity finesse provide information that is similar to the T_1 (population decay) and T_2 (dephasing) time measured in coherent spectroscopy, respectively. The time-domain ring-down experiment only measures intensity decay rates and is thus equivalent to a T_1-measurement. The measurement in the frequency domain is phase sensitive and thus equivalent to a T_2-measurement.

The level repulsion phenomena described in this Chapter, which we also observed for several sets of other mirrors, give our system the flavor of a chaotic system [42]. This is not really surprising when we think of the (imperfect) mirror as a deterministic random scatterer. Although the experiments show level repulsion qualitatively, we cannot prove chaos to its full extent.

In conclusion, we have demonstrated mode coupling in a passive resonator. The coupling changes the eigenmodes and eigenfrequencies, which no longer coincide at frequency-

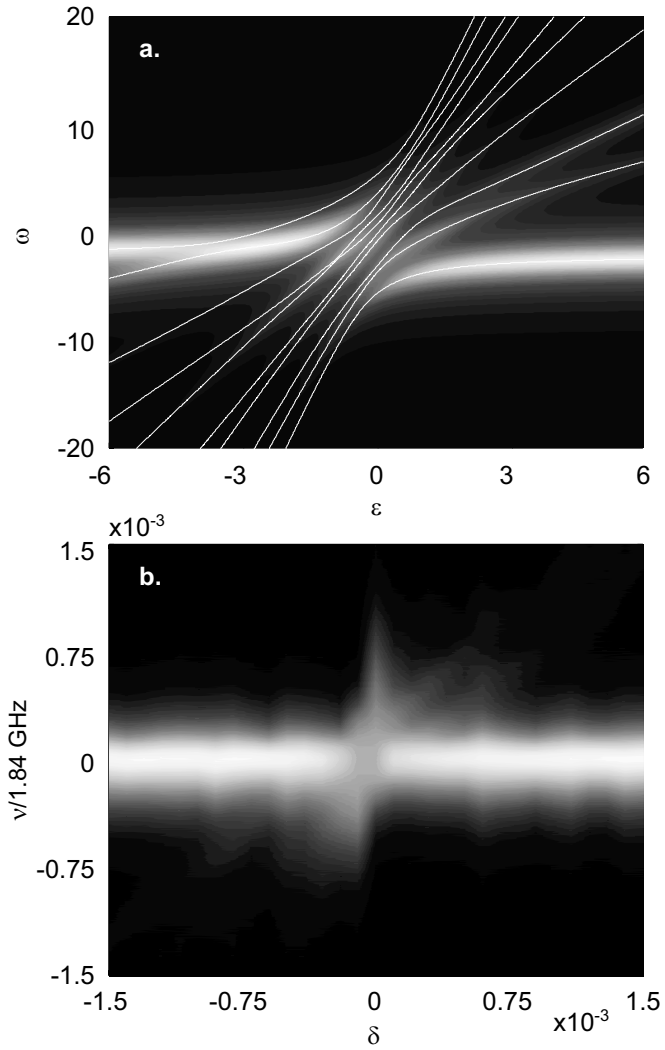

Figure 3.2: *False color (white=high and black=low) plot of the cavity transmission as a function of the normalized frequency detuning (horizontally) and frequency (vertical); vertical cuts represent transmission spectra at fixed cavity length. Both (a) simulations and (b) experimental data show how mode coupling leads to a spectral broadening and a reduction in peak transmission around the frequency-degenerate point $\varepsilon = \delta = 0$. Both effects result from level repulsion and mode mixing.*

degeneracy. This results in an inhomogeneous broadening of the measured resonance and explains the difference between the finesse measured in the time and frequency domain. A coupled-mode model correctly describes the observed behavior. These effects *cannot* be observed by cavity ring-down experiments; this should serve as a warning to experimentalists.

We gratefully acknowledge R. Sapienza for early work on this topic. This work is part of the research program of the "Stichting voor Fundamenteel Onderzoek der Materie" (FOM).

Appendix (unpublished material)

In this appendix, we discuss in more detail a number of topics, that were only touched upon in the previous Sections. First, we visualize how the shape of the mode changes due to mode coupling. Then, we estimate the number of modes involved in the coupling. As the "coupled" basis is unknown, we project it onto the standard eigenmodes in the "uncoupled" basis, *i.e.*, the Hermite-Gaussian (HG) modes. Finally, the nonexponential decay observed in certain cavity ring-down experiments is highlighted.

3.A Shape of the eigenmodes

We have mentioned that mode coupling also changes the shape of the eigenmodes. To quantify this statement, we have measured intensity profiles of modes behind the scanning resonator with an intensified CCD-camera (ICCD). The frequency-degenerate resonator ($N = 4$) is injected again with a beam mode-matched to the fundamental mode. When the resonator scans through a resonance in the spectrum, the ICCD-camera is triggered to image the intensity profiles. The advantage of the ICCD-camera is that the gatewidth ($\sim$shuttertime) is only 30 ns, very small as compared to the resonance width (FWHM) of ~ 10 μs. This means that we can visualize the mode profiles for a fixed cavity length.

The intensity profiles are measured at frequency-degeneracy ($\delta = 0$) and away from frequency-degeneracy ($\delta = 0.6 \times 10^{-3}$) in a symmetric cavity with $R = 50$ cm. Fig. 3.3a shows the profile away from frequency-degeneracy. We observe a nice HG_{00} intensity profile that we expect as only the lowest-order mode is excited and no higher-order modes are available. Fig. 3.3b shows the mode profile at frequency-degeneracy. There is still strong intensity in the center, but the mode profile is now highly distorted and shows a honeycomb-like or speckled structure. Also outside the region, shown in Fig. 3.3b, the intensity profile is different from Fig. 3.3a. At frequency-degeneracy, scattered light is present much further outside the on-axis region even up to 10 times the waist. This shows that light is also weakly coupled to many, many higher-order modes up to a mode number $m \sim 10^2 = 100$. We conclude that the light dominantly couples to the lower-order modes, but also somewhat to higher-order modes as long intensity tales are present far away from the intensity center.

3.B The number of modes involved

Now that we have demonstrated the change of the shape of the eigenmodes, and roughly know the distribution of the scattered light over the (coupled) modes, the question remains how

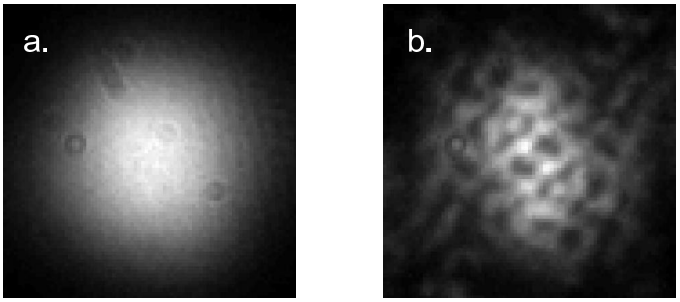

Figure 3.3: *Intensity profiles on the mirror of a resonator tuned (a) away from degeneracy and (b) at degeneracy. In both situations the cavity is injected with an (identical) input beam that is mode-matched to the fundamental mode. Away from degeneracy, we observe the fundamental Hermite-Gaussian eigenmode, whereas at degeneracy the modeprofile is totally different as the mode coupling has defined a new set of resonator eigenmodes. The dimensions of both images are* 0.45×0.45 mm^2.

many modes are involved in the coupling process. An answer to this question can be found in both the spatial and spectral domain. Measurements in the spatial domain reveal the mode number of the *highest-order* mode involved in the coupling process. Spectral measurements, on the other hand, help us to find the *effective number* of modes involved. The effective number of modes is a good measure for the number of lower-order modes involved, as light is dominantly scattered to these lower-order modes.

3.B.1 Spatial domain

In the spatial domain, the highest HG-mode that participates in the coupling can be found in two ways. First of all, it can be deduced from the spatial structure in the mode profile shown in Fig. 3.3b. The highest spatial frequency can be attributed to the highest-order mode involved. Siegman [12] states that the spatial period Λ_m of mode number m and the mode number m are related via $\Lambda_m \approx 4w/\sqrt{m}$, with w the waist of the fundamental mode. An intersection of the intensity profile shows that the lowest spatial period is $\Lambda \approx 31$ μm, which corresponds to a mode number of $m = 480$ for a waist of $w = 170$ μm. Taking into account the 4-fold frequency-degeneracy, which means that at resonance only one out of four modes is excited, we estimate for the total number of coupled modes $\sim 480/4 = 120$.

As an alternative method to determine the highest-order coupled mode, we insert an on-axis diaphragm inside the resonator. The opening of the diaphragm is increased until the intensity profile on the mirror does not change anymore. For this setting, all modes pass apparently the diaphragm. The diameter of the diaphragm $2a$ is a direct measure for the mode size. The corresponding mode m number is found from $m \approx (a/w)^2$ [12]. Experimentally, we find that for a diameter of the diaphragm of 6 mm (and higher) the spatial period remains constant. Combined with $w = 170 \times 10^{-4}$ μm, the highest-order mode has a mode number $m \sim 310$. This is roughly in agreement with the measurement based on the spatial period.

3.B.2 Spectral domain

The number of modes involved in the coupling process can also be estimated from the experimental cavity transmission shown in Fig. 3.2. More specifically, we use the width of the dip in frequency detuning $\Delta\delta$ (horizontal scale) in combination with the broadening of the normalized spectral difference $\Delta\nu/1.84$ GHz (vertical scale). This estimate from the experiment is based on, and validated by, the numerical simulation. For clarity, we note that in the experimental spectra $\Delta\delta$ and $\Delta\nu/1.84$ GHz indicate the frequency detuning and the normalized spectral difference, whereas in the numerical simulation $\Delta\varepsilon$ and $\Delta\omega$ are used.

The theoretical description centered around Eq. 3.3 is based on the assumption that all modes contribute equally to the mode coupling at $\varepsilon = 0$. For increasing ε, higher-order modes will contribute less, and modes no longer contribute if $N\varepsilon \gg c$. For small c values, only the two lowest-order modes (TEM_4 and TEM_0) couple. The width of the dip in frequency detuning $\Delta\varepsilon$ thus scales linearly with the scatter amplitude c. The broadening of the normalized spectra at $\varepsilon = 0$ is determined by the eigenvalue of a $N \times N$-matrix. Assuming equal scatter amplitudes c, $\Delta\omega$ scales with $\sqrt{N}c$ instead of c.

The number of modes involved can thus be found experimentally from the ratio of $\Delta\nu/1.84$ GHz and $\Delta\delta$ squared

$$\left(\frac{\Delta\nu/1.84\text{ GHz}}{\Delta\delta}\right)^2 = \left(\frac{\sqrt{N}c}{c}\right)^2 = N\,. \tag{3.4}$$

From Fig. 3.2b we deduce that $\Delta\nu/1.84\,\text{GHz} = 8.8\times10^{-4}$ and $\Delta\delta = 3.1\times10^{-4}$, which results in $N = 8$. The assumption that all modes contribute equally shows that light is scattered *effectively* to 8 lower-order resonant modes.

We conclude from the measurements in the spatial domain that the light is coupled to $75-120$ modes, and that the highest-order mode involved has a mode number $m = 310-480$. The coupling to the higher-order modes is, however, very weak. Spectral measurement show that light is dominantly coupled to the 8 lowest-order modes present.

3.C Cavity ring-down and mode beating

To further clarify the nonexponential decay and the mode beating in cavity ring-down at frequency-degeneracy, mentioned in Section 3.2, we demonstrate additional experimental results and introduce some theory [12]. The total field of two modes with eigenfrequencies ω_1 and ω_2 is obviously given by

$$E(x,t) = u_1(x)e^{-i\omega_1 t} + u_2(x)e^{-i\omega_2 t}\,, \tag{3.5}$$

where $u_1(x)$ and $u_2(x)$ are the spatial transverse patterns of the modes. The intensity signal that this field will produce at the detector with transverse dimension A is

$$I(t) = \int_A |E(x,t)|^2 dx = I_1 + I_2 + I_{12}\cos[(\omega_1-\omega_2)t]\,, \tag{3.6}$$

where I_1 and I_2 are just dc-currents and I_{12} is the beat frequency term, $\omega_1 - \omega_2$ being the beat frequency between the modes. The beat frequency term I_{12} equals

$$I_{12} = \int_A u_1^*(x) \cdot u_2(x) dx \begin{cases} = 0 & \text{if } A > \text{mode size} \\ \neq 0 & \text{if } A < \text{mode size} \end{cases} .$$

This integral cancels out to zero if the detector area A is bigger than the area spanned by the two modes, which have orthogonal modeprofiles. If the detector area A is smaller than the size of the modes, the modal overlap does not integrate to zero and beating occurs. The value (and sign) of I_{12} depends strongly on the size and position of the aperture in the output. Next, we will show this experimentally, for a ring-down experiment observed with a "bucket"-detector ($A >$ mode size) and a "point"-detector ($A <$ mode size) .

Away from frequency-degeneracy ($\delta = 0.6 \times 10^{-3}$), the ring-down curves in Fig. 3.4a are observed to be independent of the size of the detector. In the absence of coupling only a single mode is excited. At frequency-degeneracy, however, multiple modes will be excited with slightly different ω's. Observation of the ring-down signal with a "bucket"-detector still shows that the beating term cancels. For a "point"-detector, either on- or off-axis, the beating causes a nonexponential decay due to the level-repulsion caused by the mode coupling; this is shown in Fig. 3.4b. The decay can be faster or slower than the exponential decay, and depends on both position and size of the aperture. The reason that we observe less than one full oscillation must be that the frequency difference $\nu_1 - \nu_2$ is substantially smaller than $1/\tau \approx 3$ MHz.

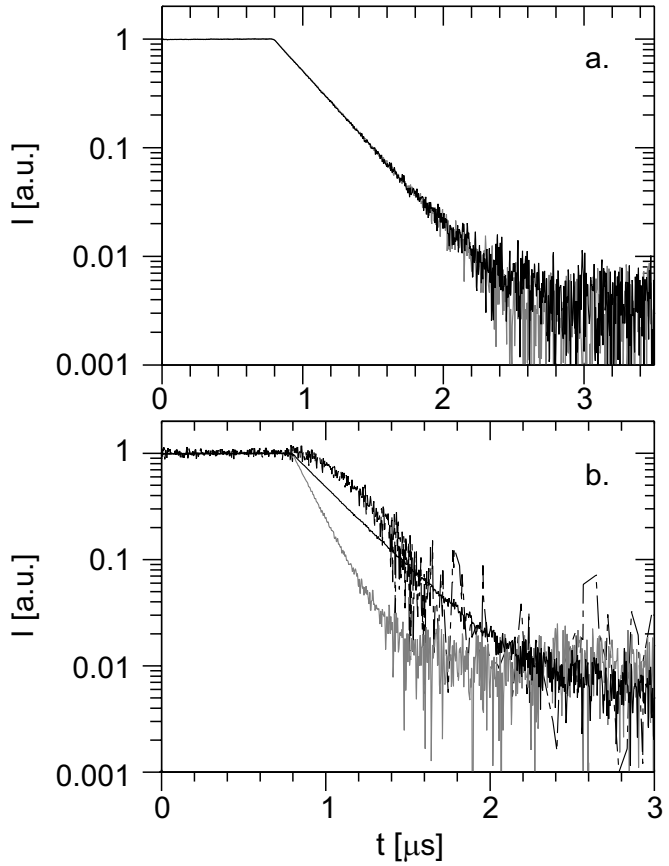

Figure 3.4: *(a) Ring-down curves of a resonator tuned $\delta = 0.6 \times 10^{-3}$ away from the ($K/N = 1/4$) frequency-degeneracy, as observed with a detector with an effective diameter of 8 mm (black) and 1 mm (grey). The ring-down curves for the "bucket"- and the "point"-detector are identical. The fitted decay time $\tau = 3.1 \times 10^{-7}$ s corresponds to a finesse $F = 1970 \pm 50$. (b) Ring-down curves at exact degeneracy ($K/N = 1/4$) for a "bucket"-detector (solid black), an on-axis "point"-detector (grey) and an off-axis "point"-detector (at $x = 0.75$ mm) (wiggly dotted). The ring-down curve for the "bucket"-detector shows an exponential decay, whereas the curves for the "point"-detectors show a nonexponential decay, indicating mode beating. The measurement of the off-axis "point"-detector is very noisy because of the low power.*